Axial Magneto-Inductive Effect in Soft Magnetic Microfibers, Test Methodology, and Experiments

Anthony B. Bruno
Ranges, Engineering, and Analysis Department

Russ Smith
NASA Langley Research Center (Structural Mechanics and Concepts Branch)

Dennis Working
NASA Langley Research Center (Advanced Materials and Processing Branch)
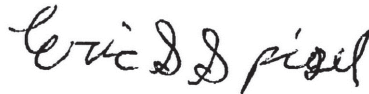
NAVSEA
WARFARE CENTERS
NEWPORT

Naval Undersea Warfare Center Division Newport, Rhode Island

PREFACE

Reviewed and Approved: 24 March 2016

Eric S S pigel

Eric S. Spigel
Head, Ranges, Engineering, and Analysis Department

REPORT DOCUMENTATION PAGE

Form Approved
OMB No. 0704-0188

The public reporting burden for this collection of information is estimated to average 1 hour per response, including the time for reviewing instructions, searching existing data sources, gathering and maintaining the data needed, and completing and reviewing the collection of information. Send comments regarding this burden estimate or any other aspect of this collection of information, including suggestions for reducing this burden, to Department of Defense, Washington Headquarters Services, Directorate for Information Operations and Reports (0704-0188), 1215 Jefferson Davis Highway, Suite 1204, Arlington, VA 22202-4302. Respondents should be aware that notwithstanding any other provision of law, no person shall be subject to any penalty for failing to comply with a collection of information if it does not display a currently valid OPM control number.
PLEASE DO NOT RETURN YOUR FORM TO THE ABOVE ADDRESS.

1. REPORT DATE (DD-MM-YYYY) 24-03-2016	2. REPORT TYPE Technical Report	3. DATES COVERED (From – To)

4. TITLE AND SUBTITLE

Axial Magneto-Inductive Effect in Soft Magnetic Microfibers, Test Methodology, and Experiments

5a. CONTRACT NUMBER

5b. GRANT NUMBER

5c. PROGRAM ELEMENT NUMBER

6. AUTHOR(S)

Anthony B. Bruno
Russell Smith
Dennis Working

5.d PROJECT NUMBER

5e. TASK NUMBER

5f. WORK UNIT NUMBER

7. PERFORMING ORGANIZATION NAME(S) AND ADDRESS(ES)

Naval Undersea Warfare Center Division
1176 Howell Street
Newport, RI 02841-1708

8. PERFORMING ORGANIZATION REPORT NUMBER

TR 12,186

9. SPONSORING/MONITORING AGENCY NAME(S) AND ADDRESS(ES)

In-House Laboratory Independent Research (ILIR) and the Office of Naval Research (ONR)
National Aeronautics and Space Agency (NASA) Langley Research Center

10. SPONSORING/MONITOR'S ACRONYM

11. SPONSORING/MONITORING REPORT NUMBER

12. DISTRIBUTION/AVAILABILITY STATEMENT

Approved for Public Release; distribution is unlimited.

13. SUPPLEMENTARY NOTES

14. ABSTRACT

Soft, amorphous, ferromagnetic microfibers under small axial tension exhibit a weak magneto-induction (MI) effect when an applied axial magnetic field is utilized to excite the fiber. Previous investigators have demonstrated this effect with small coils applied directly to the microfiber. In this report, evidence is presented that the MI effect can be generated remotely by applying a known external magnetic field from a Helmholtz coil. Excitation fields of 26 μT at frequencies ranging from 100 Hz to 1000 Hz generated a nominal 0.2 μT peak impulse response from the pre-tensioned microfiber; the axial MI response was demonstrated to be a function of the induced axial pre-tensioning. Dominant response variables include fiber length, its degree of pre-tensioning (i.e. induced strain) the magnetic field drive frequency, the applied magnetic field, and the uniformity of the applied field in aligning the domain fields within the strand. A number of fiber strand compositions were tested and mounted to dog-bone-type specimens in various ways. The results of these tests are relayed in this report, as well as a summary of results and recommendations for continued research in this area.

15. SUBJECT TERMS

Fiber, Microfiber, Magnetic, Sensor, Undersea, Deep Space

16. SECURITY CLASSIFICATION OF:			17. LIMITATION OF ABSTRACT	18. NUMBER OF PAGES	19a. NAME OF RESPONSIBLE PERSON
a. REPORT	**b. ABSTRACT**	**c. THIS PAGE**	SAR	34	Anthony B. Bruno
(U)	(U)	(U)			**19b. TELEPHONE NUMBER** (Include area code) 401-832-3206

Standard Form 298 (Rev. 8-98)
Prescribed by ANSI Std. Z39-18

TABLE OF CONTENTS

Section		Page

LIST OF ILLUSTRATIONS

Figure		Page

LIST OF TABLES

LIST OF ABBREVIATIONS AND ACRONYMS

AC   Alternating Current
DSH   Deep Space Habitat
EDS/SEM   Energy Dispersive Spectroscopy/Scanning Electron Microscope
GMI   Giant Magneto-Impedance
HC   Helmholtz Coil
ILIR   In-House Laboratory Independent Research
LBE   Large Barkhausen Effect
MI   Magneto-Induction
NASA   National Aeronautics and Space Administration
NUWC   Naval Undersea Warfare Center
ONR   Office of Naval Research
RMS   Root Mean Square
RF   Radio Frequency
SR   Small Rail
THD   Third-Harmonic Distortion

LIST OF SYMBOLS

A	Ampere
B	Boron
Bz	Magnetic Field in z Direction
Co	Cobalt
Cr	Chromium
Cu	Copper
dB	Decibel
d_a/d_u	Ratio of Atomic Distance to Uncompensated Shell Diameter
Fe	Iron
Gd	Gadolinium
H_m	Magnetic Field, measured
Hz	Hertz
I_m	Measured Current
Mn	Manganese
N	Number of Turns
Nb	Niobium
Ni	Nickle
nT	Nano-Tesla
Si	Silicon
V	Volts
w	Exchange Energy
W	Watts
Z_m	Coil Impedance, measured
μ	Circumferential Field Direction
μT	Micro-Tesla
ζ	Ratio of Coil Length to Diameter
Ω	Ohm
°	Degrees

1. INTRODUCTION

Magneto-induction (MI) effects in soft, anisotropic, ferromagnetic microfibers were first demonstrated by Mohri and Humphrey [1] in 1984. They showed that by winding a small coil around an amorphous ferromagnetic microfiber they could exhibit the MI effect. In subsequent research, Mohri and Humphrey demonstrated that MI was created by a Large Barkhausen Effect (LBE) [2-4] of reversing magnetic domains caused by a smooth magnetic force. A smooth magnetic force would be applied by a small coil wound on the magnetic fiber and a sinusoidal signal applied to the coil. Subsequent research focused on applications related to incorporating amorphous ferromagnetic microfibers into sensor circuits either through the bias coil approach or by applying a current directly through the fiber. In either case, the microfiber became part of a sensor circuit that required either batteries or other external power sources to operate the sensor. In the study detailed in this report, it was demonstrated that the fiber can be stimulated remotely using an applied magnetic field with no external circuitry or power connected to the fiber. However, a small amount of tension (1 to 15 grams) was necessary to observe the MI effect.

MI is achieved by passing an AC current through a wire, ribbon, thin film, or strip of amorphous ferromagnetic material. The passing AC current forces an alternating circumferential alignment of the magnetic domains for the corresponding wire, strip, etc. This periodic domain alignment gives rise to a nonlinear oscillation that appears at the frequency of the driving current, but is an impulsive wave train that is rich in harmonic structure. Mohri [5] noted the usefulness of this effect and identified the several classes of amorphous ferromagnetic materials that should exhibit the MI effect. Mohri and Humphrey also demonstrated that a small coil wound around the microfiber produces an axial MI effect as long as the microfiber is under a few grams of tension. Recently, Mee [6] observed that the axial MI effect could be excited wirelessly. If the axial MI effect holds true, then microfiber sensors could be fabricated to operate in many applications and environments where wireless interrogation of a passive sensor state will have a huge advantage over sensors that require interconnecting circuitry and associated battery power.

In extreme environments—such as undersea or space—wireless interrogation of a passive sensor provides an enormous advantage over sensors that require interconnecting circuitry and associated power sources, which have large mass penalties and or time limits (such as battery power). Under these conditions, microfiber sensors have many applications in structural health monitoring, weapons status during storage, biometrics, trace chemical monitoring, pressure, and more.

The National Aeronautics and Space Administration (NASA) Langley teamed with NUWC Division Newport to explore the application of microfiber sensors for the health monitoring of Deep Space Habitats (DSH) [7], which could have individual modules constructed from metallic, composite, or inflatable fabric-type materials. Of particular interest are inflatable structures, which have various construction approaches, but with a notional minimum stowed-to-deployed volume of 10 to 1 (terrestrial ratios are even better at about 20 to 1), so they are ideal for volumetrically-efficient applications in space. A smart sensor for structural integrity is needed to support vehicle development and a 2-inch-long, 30-micron-diameter microfiber sensor is ideal for this application [8].

2. TECHNICAL BACKGROUND

Amorphous ferromagnetic microfibers comprised of three different alloys (Fe_xNi_y, Fe_xCo_y, and Fe_xCr_y) are soft magnetic materials drawn into a fiber via the melt-extraction process and have average diameters of approximately ~30 μm. The percentage of Fe is typically 4% to 5%, while the percentage of the other main metal is >80 %, with the rest of the composition being Si, B, and other trace elements. They fall into a class of materials characterized as soft in that they are easily driven into saturation by low-level AC magnetic fields, typically 0.5 to 1.0 Gauss (50 to 100 μT). By way of comparison, the Earth's average magnetic field is 50 μT. A unique feature of these materials is that under low-axial tension, the non-linear response of the fiber to externally-applied AC magnetic fields is impulsive, with the pulse amplitude related to the amplitude of the axial tension.

However, the axial MI response of the fiber is two orders of magnitude smaller than the drive field (26 μT as compared to 0.2 μT), so a method to suppress the drive field is necessary to measure the fiber's axial MI response. With the drive field suppressed, the axial MI fiber response can then be measured with a small pick-up coil. The amplitude of the axial MI signal is related to the axial tension in the fiber and can therefore be used to determine the state-of-health of a structure within which the microfiber is mounted or installed. To enhance the fiber's response, the fiber must be installed in the material in a pre-tensioned state. As the tension in the fiber changes, the material response to an applied magnetic field changes in a slightly non-linear fashion; a typical fiber response is shown in figure 1. A 600x micrograph of the FeCo fiber used in figure 1 is shown in figure 2. As can be seen in the electron micrograph, the fibers are not perfect cylindrical wires but have some variability due to the manufacturing (melt extraction) process.
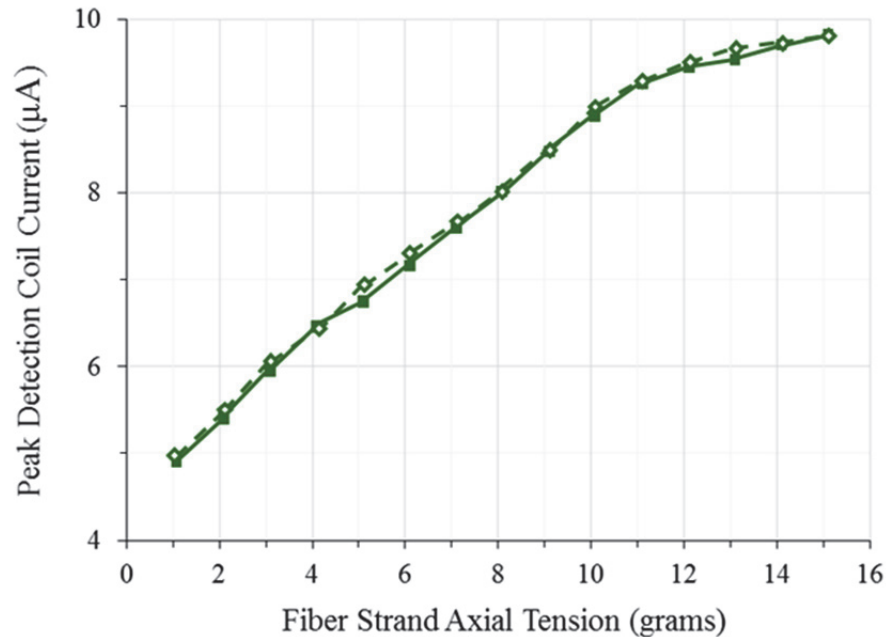
Figure 1. Nonlinear Response of FeCo Microfiber Strand
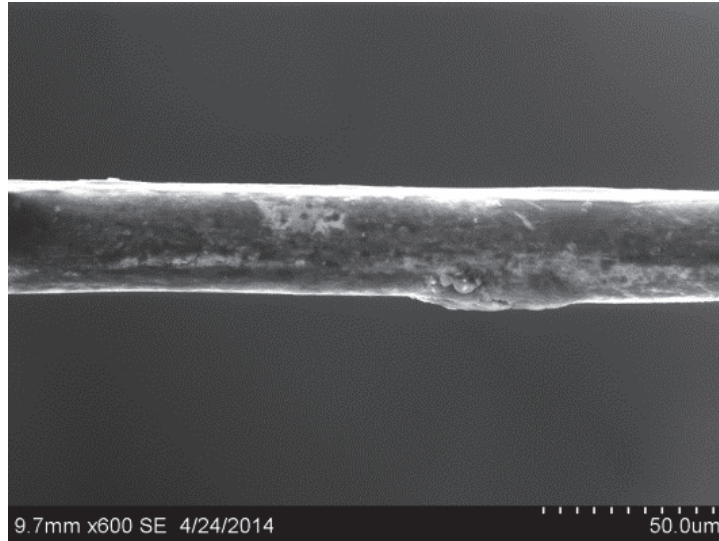
Figure 2. Electron Scan (x600) of FeCo Fiber (shown in figure 1) [6]

The melt extraction process [9–10] involves a rotating molybdenum, or ceramic disk, and a heated rod composed of the base material. The rod is heated via a microwave beam and brought into close contact with the spinning disk. As the material is spun off the disk, it is quenched with water to fix the magnetic properties of the microfibers. Individual fibers of approximately 30 microns in diameter are spun off as a bundle of microfibers with each strand being 2-to-3 meters in length. Figure 3 shows the technique as well as photographs of microfiber bundles as they are spun off by the process. Individual fibers are then separated and put on spools for distribution.
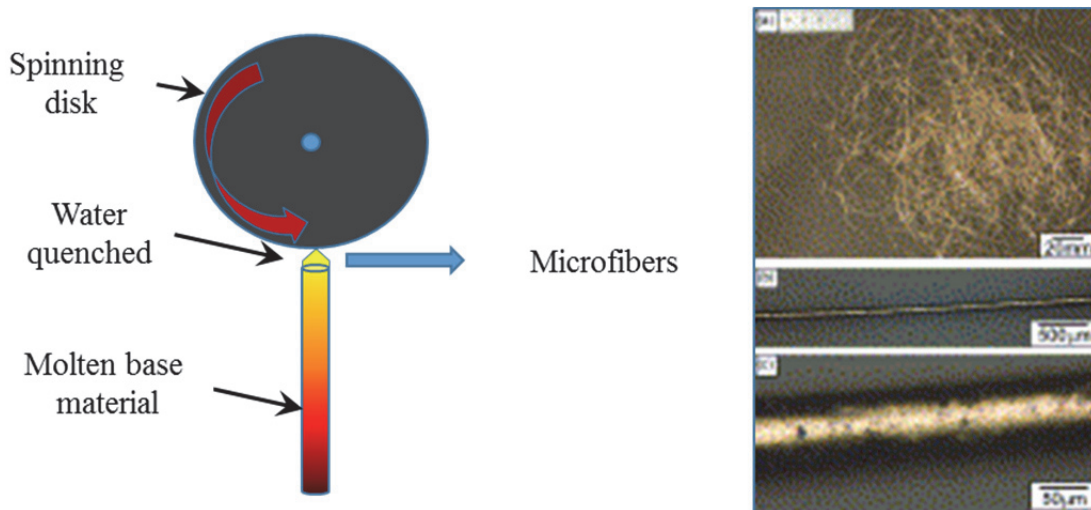
Figure 3. Melt Extraction Manufacturing Process for Microfibers

4

3. THEORETICAL BACKGROUND

Ferromagnetism arises from the magnetic moments of the individual domains of atoms, where the magnetic properties of individual atoms comprising those domains all align. This spontaneous alignment occurs even when there is no external applied field. The aggregate magnetic moment of all the domains in the sample have a preference for one direction. Figure 4 shows such a hypothetical material where several domains are aligned while others are not. The state described is only possible under two strict conditions: (1) the atoms forming the domains must have incomplete electron shells so that the spin momenta of the external electrons are not mutually compensated and (2) the radius of the d or f electron shell must be small compared to the lattice distance between atoms.

Figure 5 shows a Beth-Slater curve (after Becker & Döring [11]) plotting the exchange energy w, versus the ratio of atomic distance to the uncompensated shell diameter d_a/d_u. For ferromagnetism to occur, the overlapping electron shells must be large as compared to the interatomic distance. Only certain metals meet these requirements including Fe, Ni, and Co. Iron alloys of metals, such as Mn and Cr, will also meet the requirement. Under the condition of an applied magnetic field, as the field increases the domains will rotate and align with the applied magnetic field. However, the effect is not continuous, as there is a threshold applied field or equivalent current below which the domains are pinned in place. At the appropriate current, the domains rotate and oscillation will occur. The effect is known as pinning and the subsequent domain rotation is the LBE.
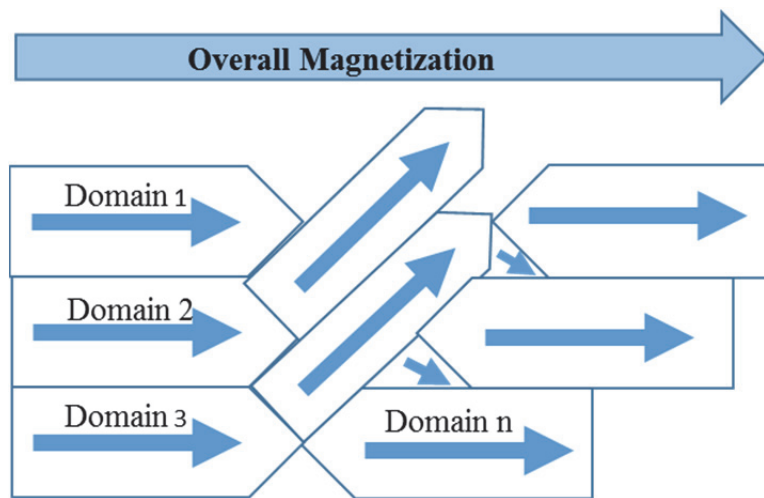
Figure 4. Hypothetical Domain Structure of Spontaneously Magnetizing Material
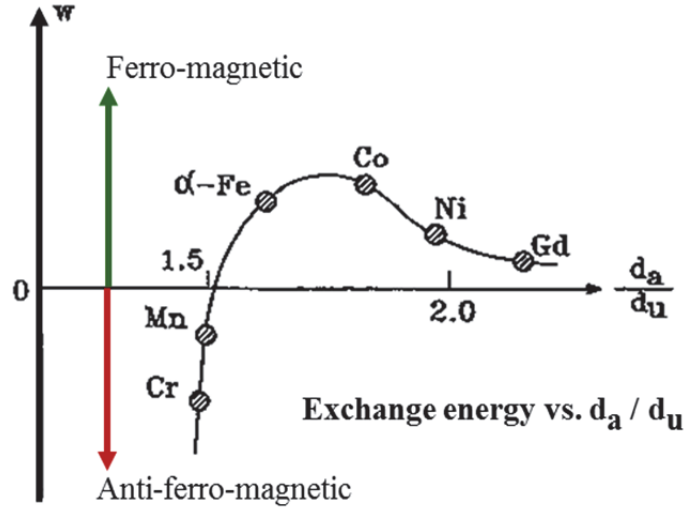
Figure 5. Exchange Energy versus d_a/d_u [12]

Domain rotations can occur in two dimensions, both in the axial direction and in the ϕ direction depending on the excitation. If the microfiber is excited by driving a current down the fiber (as in most applications) then the applied field is circumferential and the domain oscillations take place in the ϕ direction. If the field is applied via a small coil, then the oscillation is in the axial direction. Figure 6 shows a depiction of the two types of domain alignment for both types of applied fields.
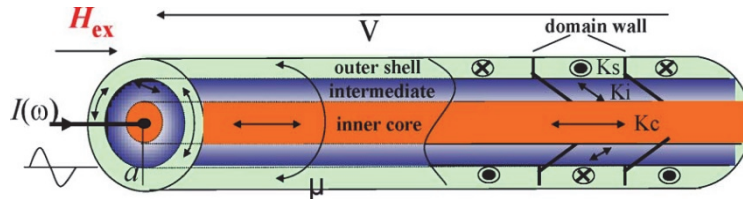
Figure 6. Domain Model of Amorphous Microfiber after Mohri [13]

Another interesting phenomena associated with amorphous ferromagnetic microfibers is the Giant Magneto-Impedance (GMI) effect. The GMI effect occurs when a radio frequency (RF) current is driven down the microfiber and a change in RF impedance is observed in the presence of an applied external magnetic field. The GMI effect is defined as,

$$GMI\ Effect = \frac{\Delta Z}{Z} = \frac{Z_H - Z_{H=0}}{Z_{H=0}} = \frac{Z_H}{Z_0} - 1$$

where H = applied magnetic field , $Z = Z_0$ is the RF impedance of the microfiber under zero field condition, and Z_H is the RF Impedance under applied magnetic field. The GMI effect is observed only at frequencies above 1.0 MHz and usually persists until cutoff, where the skin effect excludes the current density from the microfiber. Exclusion is property-dependent and the GMI effect has been observed to increase up to 335 MHz for the $Fe_{5.3}Co_{81.8}$ microfibers. Figure

6

7 shows laboratory measurements of the GMI effect up to 500 MHz. In the present study, samples of microfiber from different batches were measured, but all were believed to be of similar composition. Three samples were found to exhibit the GMI effect and three had no GMI effect. Table 1 shows the sample numbers and observed properties of selected specimens; all of the samples have major constituents comprised of $Co_{81.8}Fe_{5.3}Si_{9.0}Nb_{3.9}$.

Earlier investigators (Ciureanu [14]) have noted major differences in the MI circumferential response between the microfiber samples that were measured, but this has not been confirmed. Mee [15] has also reported variations in the MI axial response from the same group of microfibers. None of these variations have been correlated with compositional variations from the original samples. To solve the mystery, NASA Langley [16] performed Energy Dispersive Spectroscopy/Scanning Electron Microscope (EDS/SEM) on all of the microfiber samples to determine their crystalline properties. A typical mass spectroscopic plot from the control sample is shown in figure 8. In the present work, only axial domain excitation of the MI effect at low frequencies was studied.
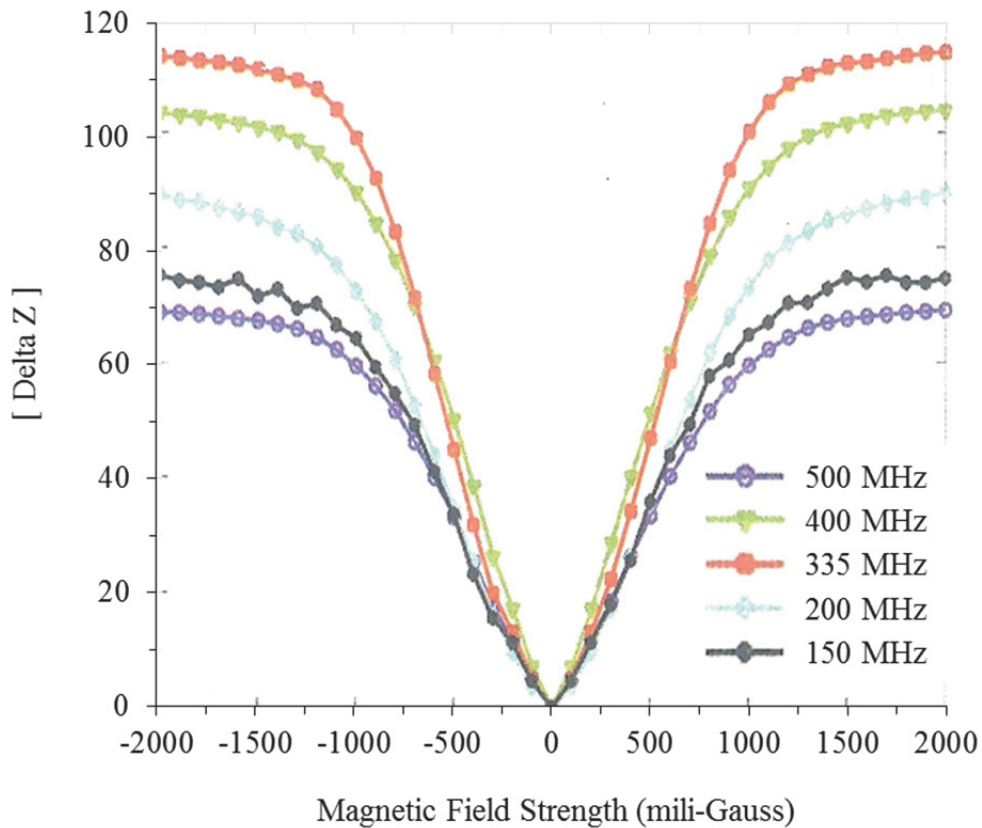
Figure 7. GMI Measurements up to 500 MHz

Table 1. Microfiber Samples and their As-Manufactured Lot Numbers

Sample #	Lot # (for reference)	GMI Effect
1	290200-01	Yes
3	000003-01	Yes
4	CHO-240899-01-075	Yes
8	061101-02	No
10	CHO-300402-01-040	No
12	191101-01	No
Note: fiber sample #12 is the control specimen		

Element	Weight %	Std. Dev.
Co	81.8	0.2
Si	9.0	0.1
Fe	5.3	0.1
Nb	3.9	0.2
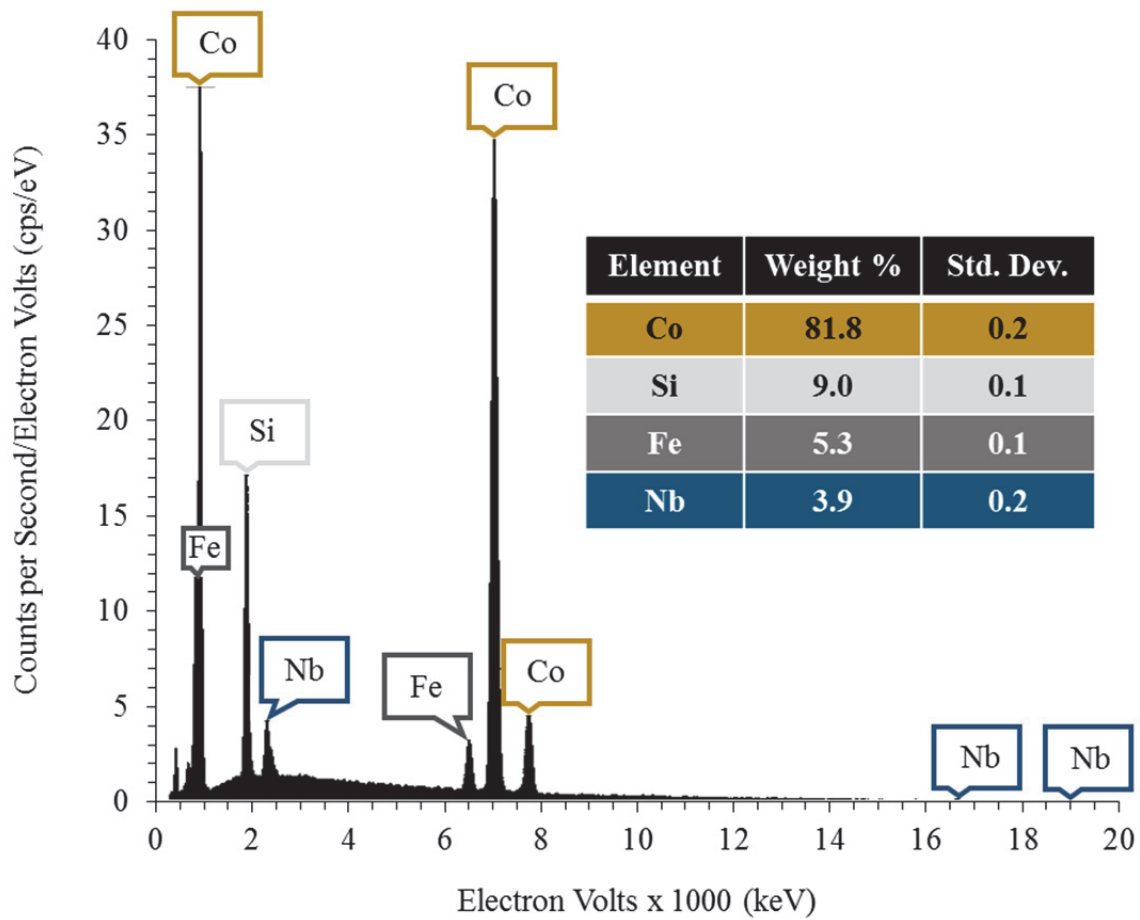
Figure 8. Mass Spectroscopic Analysis of the Control Sample after NASA [16]

4. MEASUREMENTS AND EXPERIMENTAL APPARATUS

A controlled and repeatable source for a magnetic field was required and a method to cancel the high excitation, or drive field, was necessary to observe the axial MI effect. A Helmholtz Coil (HC) is a device used to generate controlled, calibrated, and uniform AC fields within a specific volume. Due to limited resources, existing HCs were tried until one that provided the appropriate field—and could also be matched properly to a power amplifier—was selected. Subsequently, a measuring system had to be devised that would have sufficient sensitivity to measure the axial MI effect and simultaneously remove the very high excitation field. In addition, a method for applying pre-stress to the microfiber samples needed to be developed. This method also needed to allow the pre-stressed samples to be inserted into the HC for exposure to a magnetic field with a uniform region of field excitation (i.e. smooth magnetic force) while simultaneously subtracting the excitation field, without removing the signal of interest.

Figure 9 shows an 8-inch-diameter HC that was used for the initial measurements. A HC consists of two identical coils of equal turns that are wired in series. The two coils are spaced such that the separation between the two coils is equal to the radius of the individual coils. When a current flows through the two coils, the magnetic field associated with that current is uniform along the axis between the two coils, but diverges rapidly outside the coils.
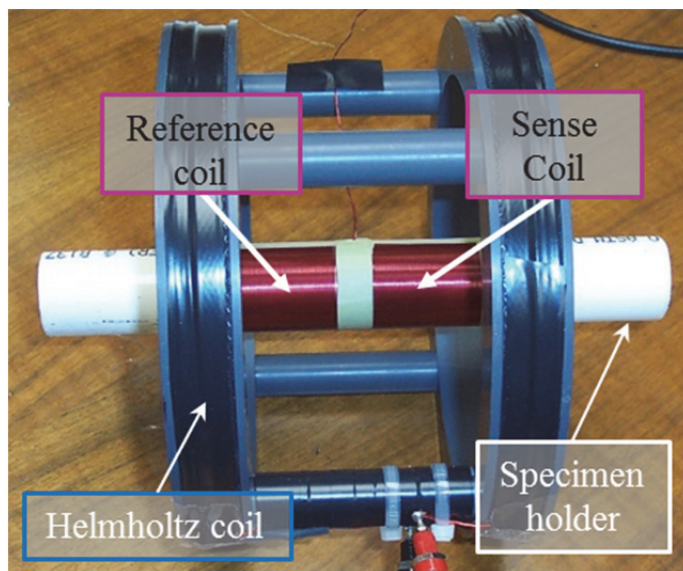
Figure 9. Microfiber Measurement System

An image of this magnetic field is shown in figure 10, where the X and ● represent the current's direction of flow in the HC and the black lines with arrows represent the magnetic field supported by those currents; note that the field is uniform between the coils, but diverges rapidly outside the coils. This arrangement is ideal for generating an axial field to excite the microfiber.

Once again referring to figures 9 to 10, a measurement coil consisting of a sense coil and a reference coil is shown inside the HC and aligned along its axis. As detailed, the measurement coil consists of two identical solenoids with 106 turns of copper magnet wire. However, the two coils are wired in opposition (i.e. opposite directions), such that the HC field signal induced in each of the measurement coils is cancelled. The microfiber is positioned inside the sense coil such that the axial response of the microfiber can be measured but the larger excitation field of the HC is cancelled.

This arrangement of sense coil and reference coil has proven to be effective in cancelling the drive field while measuring the microfiber response field. However, there are some limitations due to the size and spacing of the measurement coils within the HC as well as the separation between the reference coil and the sense coil. To achieve maximum cancellation, the reference coil and sense coil must be entirely within the uniform region of the HC and the separation between the reference coil and the sense coil must be large enough to prevent a portion of the microfiber signal from appearing in the reference coil.

Figure 10 shows this relationship between the coils in a highly-exaggerated representation of the fields as they interact with each coil. Any portion of the sense coil or reference coil outside of the linear field region will introduce errors into the measurement of the microfiber signal. To resolve the measurement difficulties introduced by the 8-inch-diameter HC, it was concluded that a larger HC would be required.
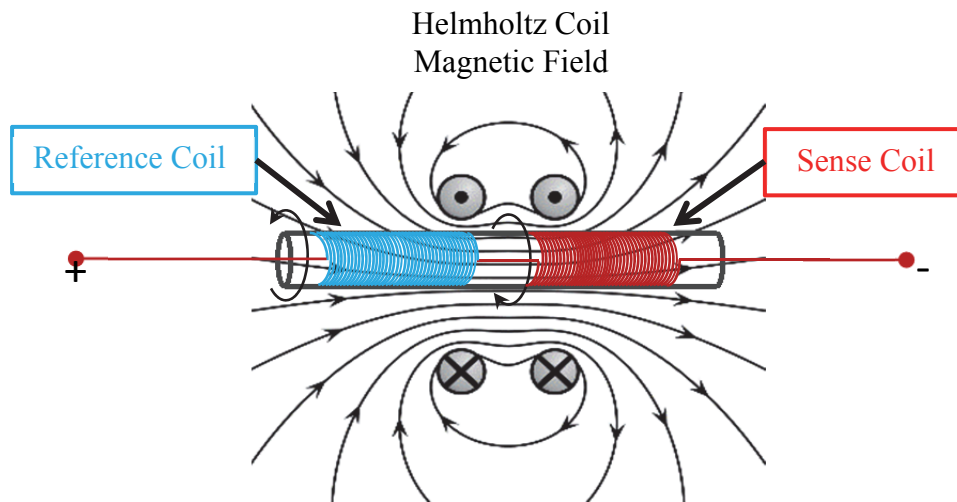
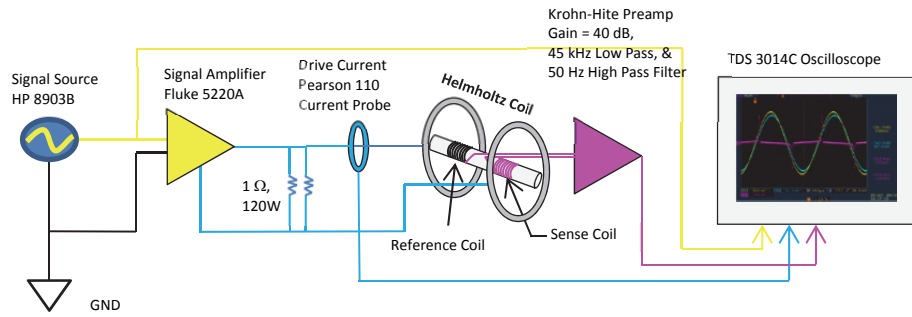*Figure 10. Magnetic Field of the Helmholtz Coil with Reference and Sensing Coil(s)*

Figure 11 shows the equipment used to generate the known input field in the HC (source equipment) and the signal measurement equipment that is needed to detect the microfiber signal in the sense coil.
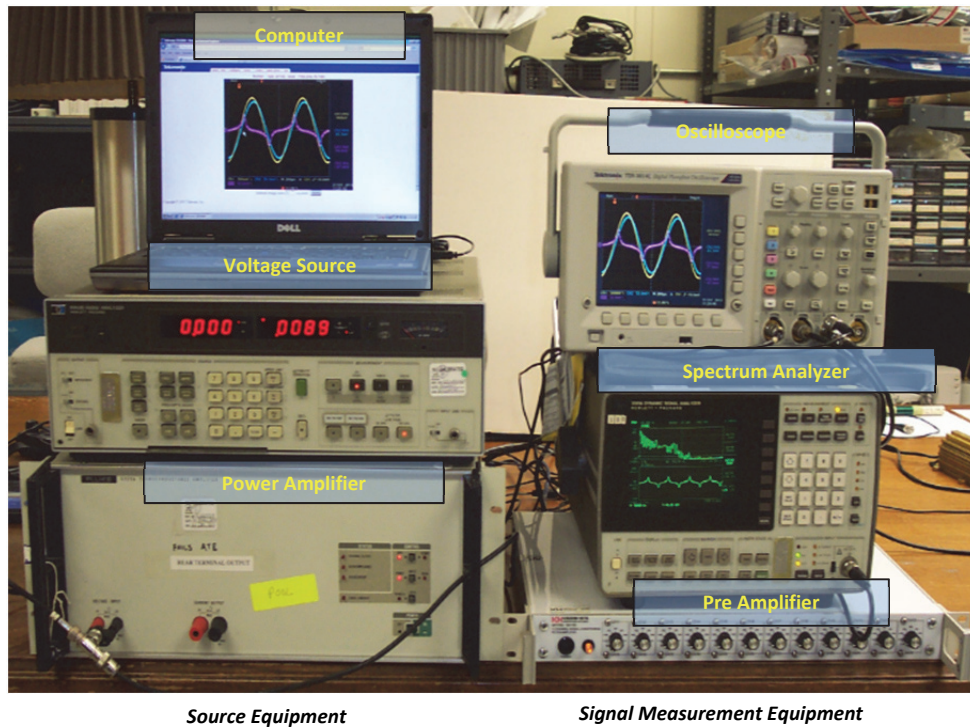
Figure 11. Microfiber Source and Measurement Equipment

The system block diagram (figure 12) is color coded by function: yellow for the drive voltage, light blue for the drive current, and magenta for the microfiber signal. Low-distortion sine waves (with third-harmonic distortion (THD) better than −90 dB) are generated by the signal source, an HP 8903B Audio Analyzer. The input sine wave is amplified by the constant current power amplifier (a Fluke 5220A Conductance Amplifier) i.e., 1 volt input gives 1 ampere output. The input current is measured by a Pearson 110 wideband current probe (0.1 V = 1 A).

The input current feeds to the input of the HC, which produces a uniform axial magnetic field in line with the microfiber axis. From the measured input current, the magnetic field inside the HC can be computed from the known HC constant i.e., 33 mA/μT. Once the magnetic field reaches its threshold, the microfiber oscillates between two states: + and − in phase with the HC's magnetic field (the field lags the current by $\pi/2$). The magenta line in figure 12 shows the output of the sense coil, preamplifier, and oscilloscope trace of the MI signal from the microfiber. The oscilloscope measures the peak voltage of the microfiber signal and captures the signal waveform for further analysis. Applying the known gain of the preamplifier gives the peak voltage measured at the output of the sense coil. The 1 Ω shunt resistor is needed to stabilize the load of the conductance amplifier.

Signal Source
HP 8903B

Signal Amplifier
Fluke 5220A

Drive Current
Pearson 110
Current Probe

Krohn-Hite Preamp
Gain = 40 dB,
45 kHz Low Pass, &
50 Hz High Pass Filter

TDS 3014C Oscilloscope

Helmholtz Coil

1 Ω,
120W

GND

Reference Coil

Sense Coil

Figure 12. Measurement System Block Diagram

5. SAMPLE PREPARATION

Smith and Working [17] devised a simple method of applying pre-stress to microfiber samples in standard dog-bone test fixtures. The microfibers are sandwiched between two halves of Surlyn (a self-healing polymer blend) in a groove etched down the axis specifically to accommodate the microfiber; a small weight was then applied to create the appropriate pre-stress. The samples are then either bonded together, or the microfiber is taped to the Surlyn substrate dog bone. Figure 13 shows a design sketch of this specimen construction procedure, while figure 14 shows the dog-bone microfiber samples ready for testing.
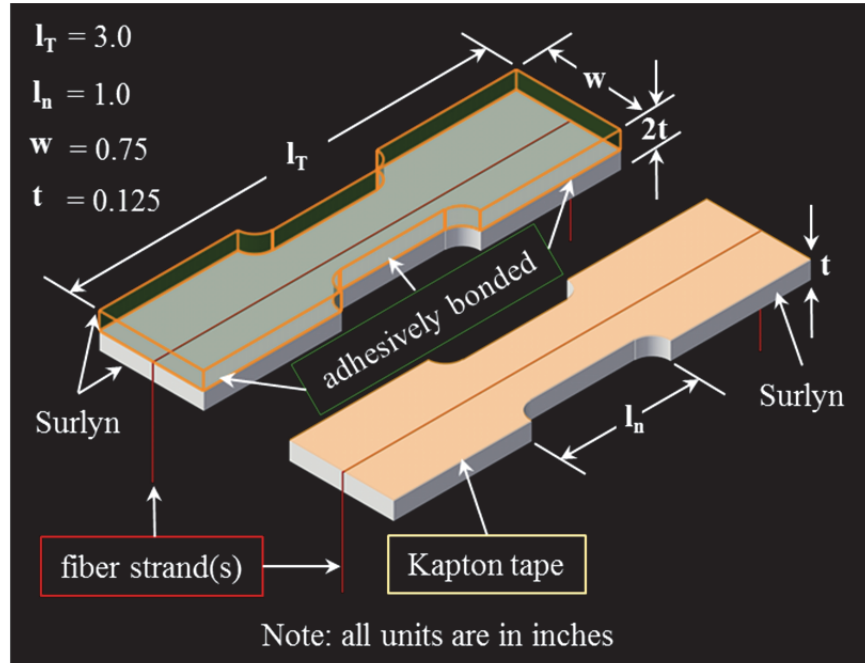
Figure 13. Dog-Bone Sample Construction after Smith and Working [17]
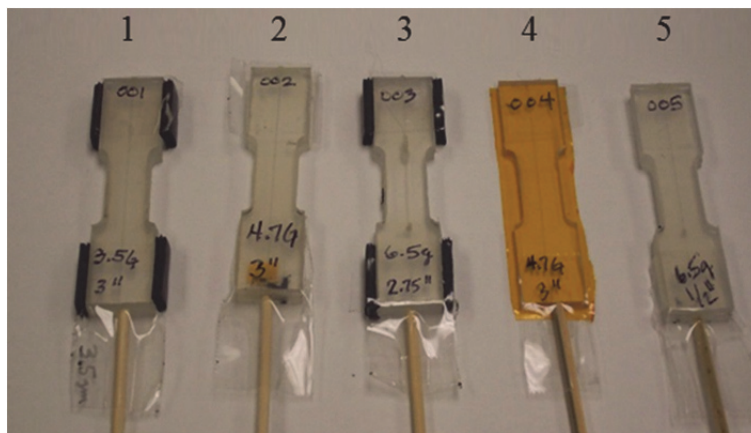
Figure 14. Dog-Bone Samples with Pre-Stressed Microfiber Strands

More specifically, samples were bonded between two Surlyn dog bones with 3M Scotch Weld structural adhesive, except for one sample that was taped with Kapton high-end tape. All samples were pre-stressed with 3.5 to 6.5 grams of dead weight. Table 2 lists the specific details for each dog-bone sample. All microfiber samples were similar and were from microfiber sample 12 control number 191101-01 (see table 1).

Table 2. Microfiber Test Samples

Sample #	Pre-Stress (grams)	Fiber Length (inches)	Epoxy or Tape	Threshold (Volts)
1	3.5	3	Epoxy	0.12
2	4.7	3	Epoxy	0.15
3	6.5	1	Epoxy	0.45
4	4.7	3	Kapton	0.17
5	6.5	2.75	Epoxy	0.10

Notes on Table 2:

Sample 1: 5-inch wire, 3.5 grams full length.

Sample 2: Full-length sensor wire is 3.73 inches at 4.7-grams pre-stress using Scotch Weld Epoxy adhesive DP460NS.

Sample 3: Sensor wire under tension is 2.75 inches at 6.5-grams pre-stress. Last in gauge length.

Sample 4: Tape 3.5-inch sensor wire at 4.7-grams pre-stress using Kapton Tape (3M Scotch brand).

Sample 5: Half-length sensor wire (at 2.75 inches) with 0.038 hole at 6.5-grams pre-stress using Scotch Weld Epoxy adhesive DP460NS.

6. MEASUREMENT RESULTS

All five test specimens were measured with an 8-inch HC and all microfibers were from original lot number 191101-01; $Co_{81.8}Fe_{5.3}Si_{9.0}Nb_{3.9}$, with a nominal diameter (d) = 34 μm. Measurements taken at 100, 500, and 1000 Hz at a 1-volt input, with a current (I) output at 877 mA and which generated a drive field = 26 μT. The identified threshold voltage to initiate de-pinning was $V_t > 0.10$ V. For voltages > the minimum, the axial magnetic field is large enough to overcome the molecular resistance between domains and initiate oscillation within the material; this effect is known as the MI effect and de-pinning refers to the natural domain resistance to the MI oscillation. All data were captured electronically to facilitate further analysis. See table 2 for the threshold voltages necessary for each sample to overcome de-pinning.

Figure 15 provides the dataset with input voltage, drive current, and microfiber response shown for each sample at three different frequencies. Input voltage is plotted in yellow, drive current in blue, and microfiber response in magenta. Table 3 provides a summary of the measured data for each microfiber sample versus frequency and tension. Also, table 3 includes the root mean square (RMS) values for input voltage (mV) and input drive current (mA). Measured microfiber peak response is in ± mV. Also shown in brackets, [ ], in column 5 is the average peak response of the microfiber (mV). In general, the following observations are applicable to table 3 and figure 15: all output signal levels have +40-dB Gain (factor of 100), all samples were measured at room temperature, and all samples were measured at the same orientation relative to magnetic north. Each microfiber responded to the input magnetic field as shown in table 3. General observations include: microfiber output increases with increased frequency, microfiber output increases with increased fiber length, and microfiber output increases with increased pre-stress.
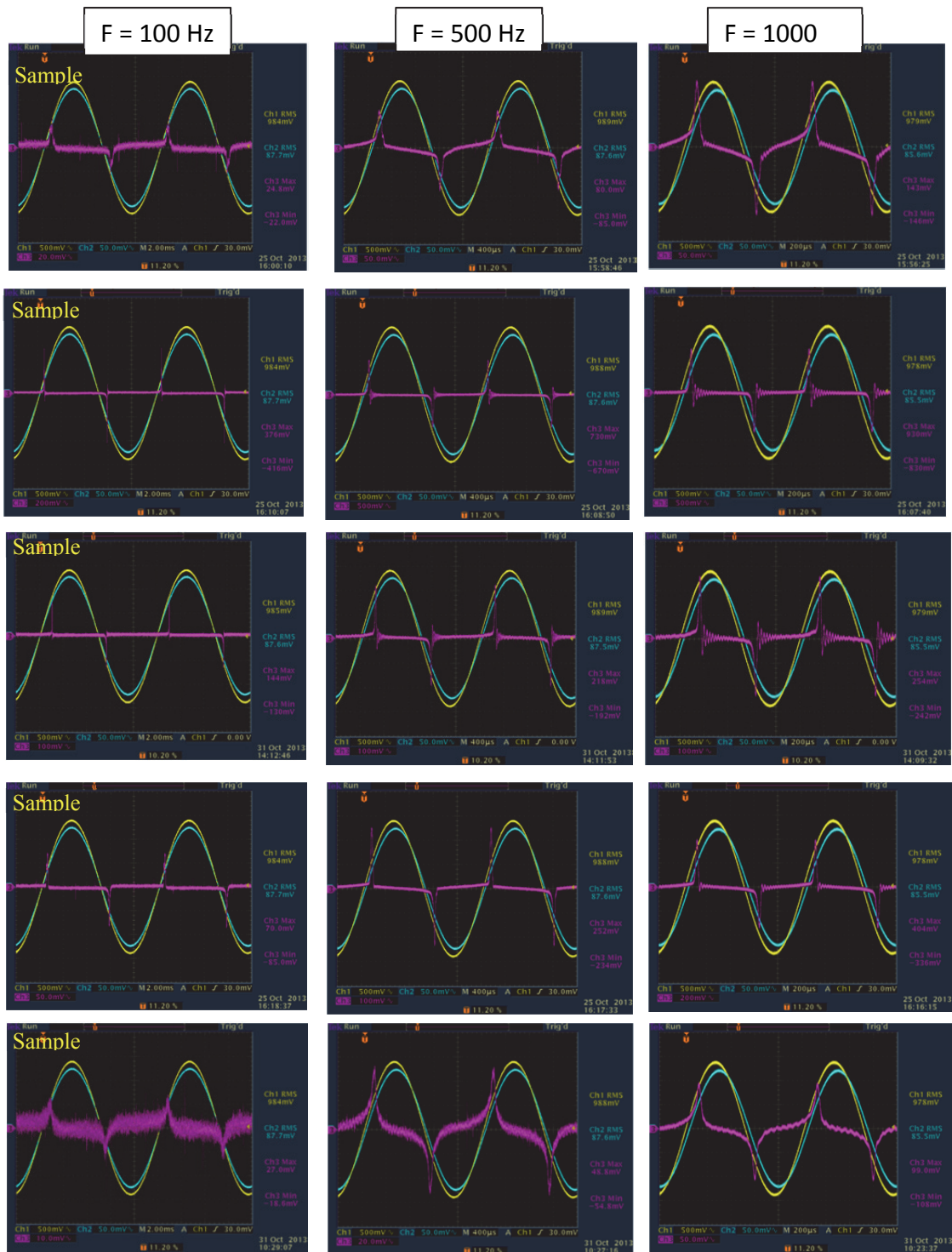
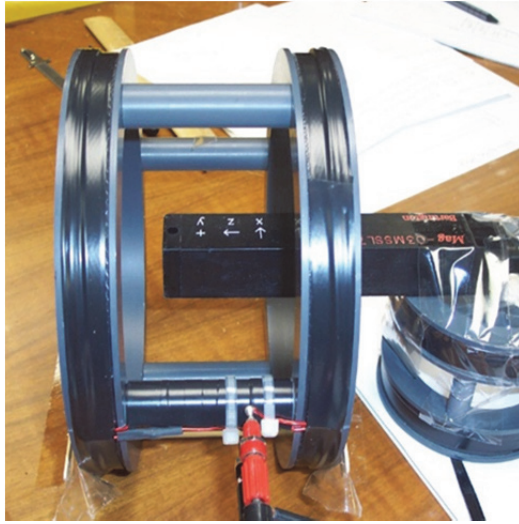***Figure 15. Microfiber Responses at Various Frequencies***

Note: In figure 15, yellow trace input voltage 500 mV/div; blue trace input current 50 mV/div; magenta trace microfiber response scale variable to give best signal. See table 3 for details.

16

Table 3. Microfiber Peak Response versus Frequency

Sample #	Frequency (Hz)	Input Voltage (mV)	Output Current to HC (mA)	Microfiber Peak Response ± (mV) and average response [mV]
1	100	984	877	25 / −22 [24]
1	500	989	876	80 / −85 [83]
1	1000	979	856	143 / −146 [145]
2	100	984	877	376 / −416 [396]
2	500	988	876	730 / −670 [700]
2	1000	978	855	930 / −830 [880]
3	100	985	876	144 / −130 [137]
3	500	989	875	215 / −192 [204]
3	1000	979	855	254 / −242 [248]
4	100	984	877	70 / −85 [78]
4	500	988	876	252 / −234 [243]
4	1000	978	855	404 / −336 [370]
5	100	984	877	27 / −19 [23]
5	500	988	876	49 / −55 [52]
5	1000	978	855	99 / −108 [104]

Figure 16 shows the calibration measurements used to estimate the coil constant (mA/μT) for the 8-inch HC. The data were taken with a Bartington Mag-03MSS three-axis reference magnetometer. The magnetometer is placed inside the HC with the sensor's measurement axis lined up with the axis of the HC and then centered to minimize off-axis components (as shown in the figure 16a). Subsequently, data were taken at 100, 500, and 1000 Hz over a range of input currents and plotted in figure 16b. The average coil constant was found to be 33.2 mA/μT. The coil constant is used to estimate the input magnetic field of the HC that is needed to excite the microfiber. The average excitation field for the sample data was 26.2 μT.
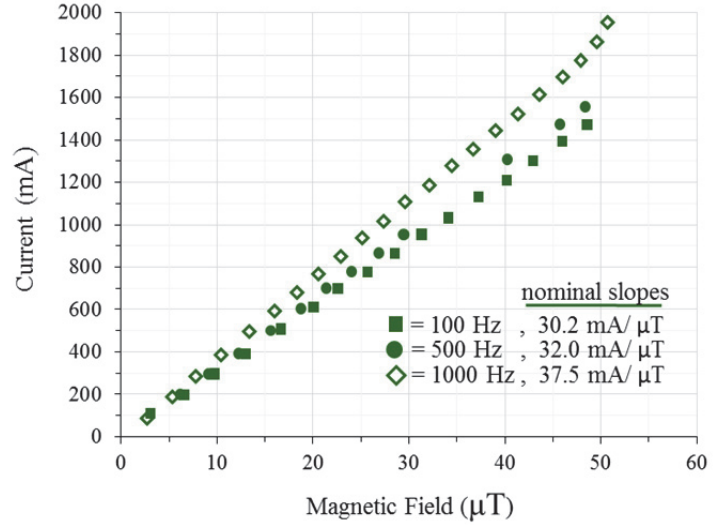
(a) HC Calibration

(b) Data and Nominal Slopes versus Frequency

Figure 16. Helmholtz Coil Calibration, and Data, at Various Frequencies

To estimate the response field of each microfiber sample, the measured coil output in mV is taken from table 2, adjusted for system gain, and then used to compute equivalent current, I_m. $I_m = V_m/Z_m$ is computed from measurements of the coil impedance at the various frequencies. For the three frequencies, the measured impedance Z_m are given in table 4. Then, using the formula for the magnetic field of a thin solenoidal coil,

$$B_z = \frac{NI_m}{2b}\frac{\zeta}{\sqrt{1+\zeta^2}} \tag{1}$$

where $N = 106$ turns, I_m is the equivalent measured current, $\zeta = b/a$ where $2b = 2$ inches is the coil length, and $d = 2a = 1.315$ inches is the diameter of the measurement coil. Measurements were performed with an HP 4192A Impedance Analyzer. Estimates of the microfiber's equivalent magnetic field for each sample at the measured frequencies are in table 5.

18

Table 4. Measurement Coil Impedance

Frequency (Hz)	Magnitude (Ω)	Phase Angle (deg)
100	3.55	3.87
500	3.74	19.09
1000	4.30	34.77

Table 5. Microfiber Equivalent Magnetic Field versus Frequency

| Sample	B_z (nT) at f = 100 Hz	B_z (nT) at f = 500 Hz	B_z (nT) at f = 1000 Hz
1	153.1	468.7	729.0
2	2320.6	4276.5	4740.8
3	888.7	1277.1	1294.8
4	432.0	1476.3	2059.4
5	166.6	285.9	504.7

The response data for each microfiber sample shown in table 5 indicate that fields as small as 0.15 µT and as large as 4.7 µT over a range of frequencies are likely to be encountered by a probing system trying to interrogate an embedded microfiber (such as the NASA DSH). The probing field is at least 10 to 100 times larger than the response field of the specimens. In this example, excitation fields of 27 µT were used. A useful field probe, like the one utilized in this study, would be required to cancel the excitation field in order to measure the microfiber signal.

A second apparatus was constructed to measure microfiber response as a function of tension. In this experiment, an individual microfiber (2-inches long from lot number 191101-01) was assembled into an apparatus so that variable tension could be applied to the microfiber while keeping the microfiber centered in the measurement coil and within the uniform region of the HC. The 2-inch length of microfiber is spliced between two sections of 100-pound-test fish line of approximately the same diameter. The microfiber ends and fish line are epoxied together with Teflon insulation sleeves taken from a #40-gauge Cu wire. The epoxy is allowed to set overnight before tension is applied to the sample. The apparatus for applied tension is shown in figure 17.
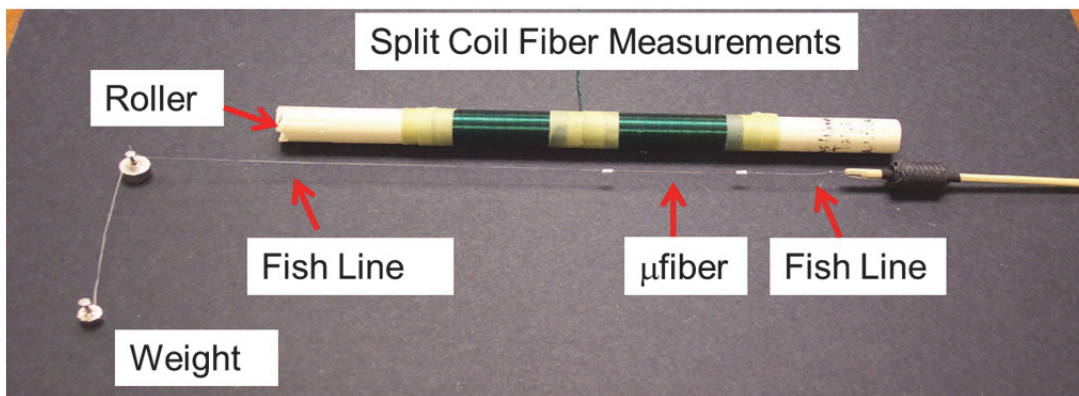

Figure 17. Apparatus for Applying Variable Tension to Microfiber Sample(s)

In figure 17, the black rubber stopper on the right self-centers the microfiber in the measurement coil, while the roller supports the fish line and transmits the tension from the weight to the sample. Figure 18 shows the measurement apparatus in the HC. In this experiment, tension was applied to the microfiber through the application of various weights ranging from 1 to 10 grams.
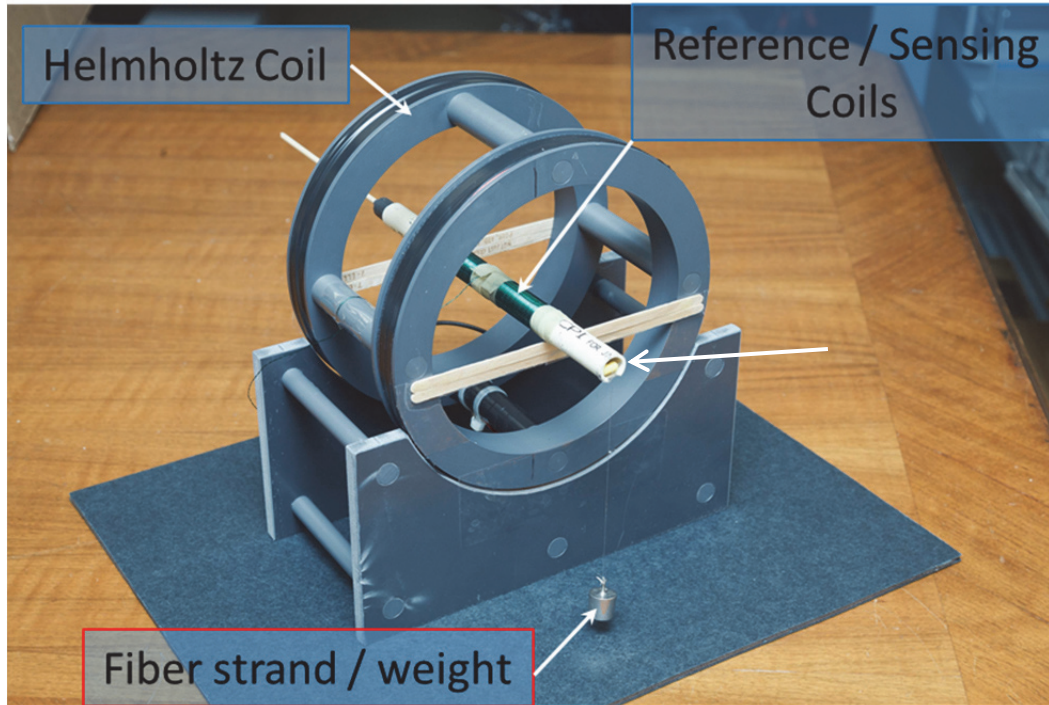
Figure 18. Microfiber Variable Tension Measurement Apparatus

The microfiber response at 500 Hz is measured in the HC with an applied field of 28.13 µT. The variable tension measurement coil has a diameter of $2a = 0.630$ inches, length $2b = 2.0$ inches, and $N = 152$ Turns. The coil impedance at 500 Hz was measured with the HP 4192A Impedance Analyzer and found to be 5.772 Ω at 6.63°. The raw measured voltage is converted to equivalent current and then equation 1 is used to estimate the equivalent fiber field as a function of applied tension; results are shown in figure 19. The linear range of applied tension appears to be from 2 to 8 grams and for this sample set; it is the useful range over which a sensor could be built. To convert grams (axial tension) as shown in the graph in figure 19 to axial stress, σ_{zz}, multiply the mass (in grams) by 13.9 to get the axial stress on the microfiber in MPascals, where the nominal fiber diameter is 30 µm.
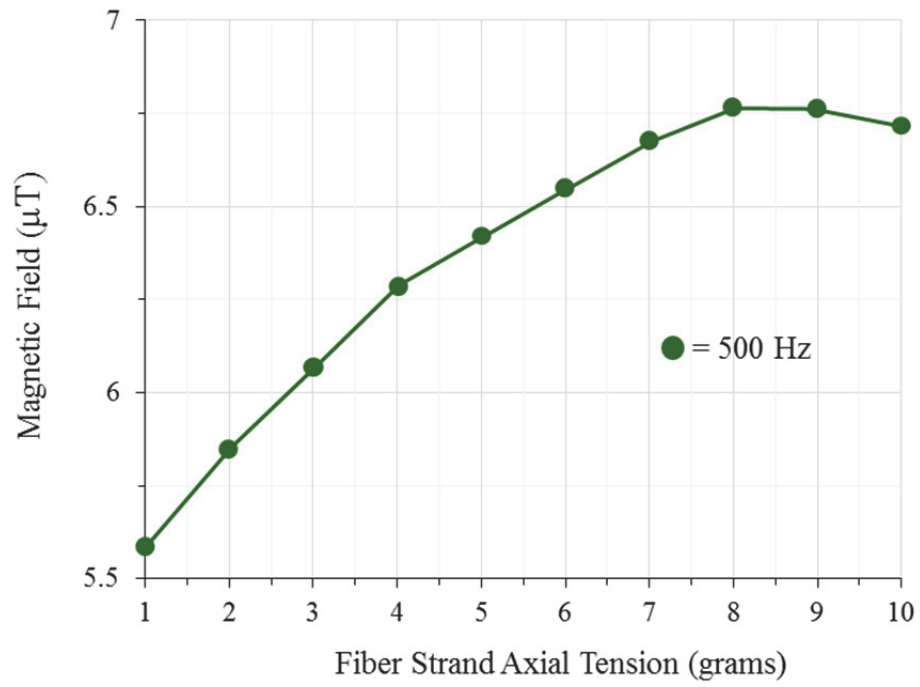
Figure 19. Tensile Microfiber Response at 500 Hz

7. RECOMMENDATIONS AND CONCLUSIONS

This report has demonstrated the potential applications of microfiber strands as embedded health monitoring sensors in composite and inflatable fabric structures. The data indicate that a device could be constructed to remotely monitor the state of a microfiber sensor and thus the overall health of a structure into which the sensor is embedded. NASA Langley is investigating the usefulness of inflatable structures for space habitats. Figure 20 shows a DSH prototype that is currently utilized for human factors studies; within the structure are various panels constructed of composite as well as fabric based structures. Within both the first and second floors was a composite fabrication prototype known as the Smart Rail (SR) system. This SR system has microfiber strands mounted to the Gate section in each story. A microfiber remote monitoring device (as demonstrated in this report) could be used to monitor the state of the Gate microfiber sensors, and thus the health of the structure.

Figure 21 shows a typical SR Gate that has a microfiber sensor attached to the structure via Kapton tape. The sensors are positioned such that if the panel undergoes a load that would either elongate or break the microfiber, then a remote measure of the microfiber's magnetic state would indicate that the fiber was disturbed. This disturbance, in turn, would indicate a potential over-stress condition associated with that panel.

2nd-Story Loft
Crew Quarters
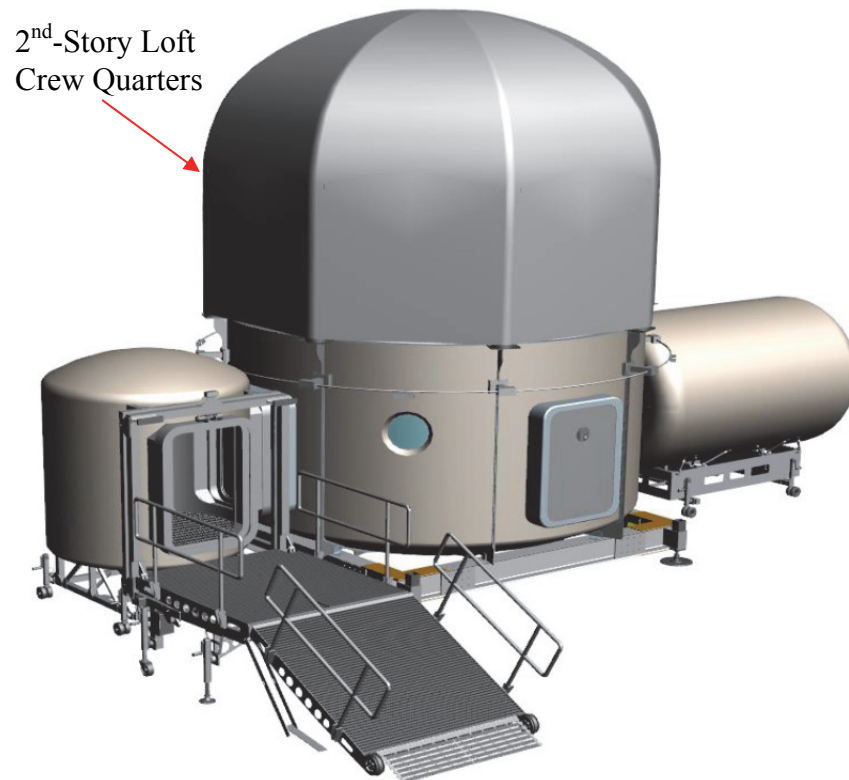
Figure 20. NASA DSH Prototype [18]
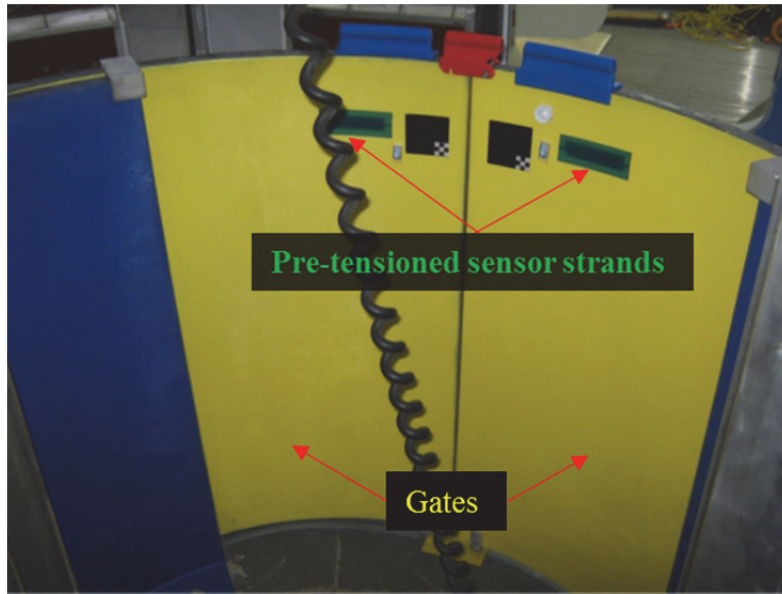
*Figure 21. Smart Rail Gate Section as Installed into the DSH with Microfiber Sensors [18]*

8. FUTURE WORK

This report has only considered one sample from the six original microfiber samples available for study. In addition, the mass spectroscopic measurements have not been compared to tension measurements that were made for each fiber. The measurement apparatus, including the HC, were too small to measure the microfiber responses without contamination from the drive field.

A good rule of thumb is to have the HC dimensions be at least three times the largest length dimension of the sample under study. In this case, the sample is the combined measurement coil and reference coil. The total length is approximately 4 inches, so the minimum HC radius should be approximately 12 inches.

A new HC with a diameter of 24 inches has been constructed and is shown in figure 22. A HC at this diameter will have a region of uniformity (smooth magnetic force) that is sufficient to get good rejection of the drive field while measuring the specimen microfiber field response.
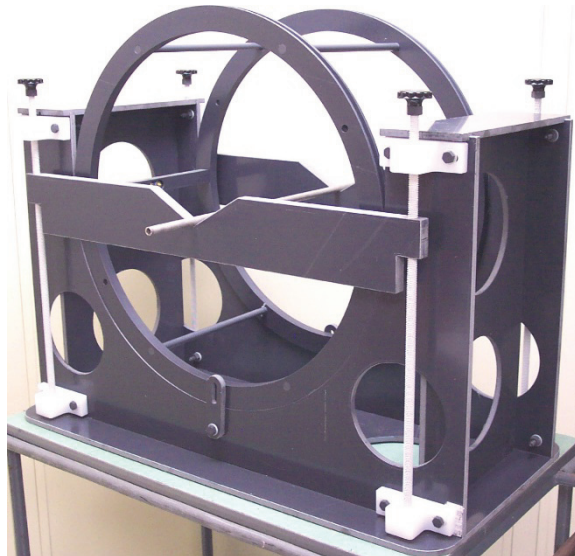

*Figure 22. New 24-Inch-Diameter Helmholtz Coil*

The apparatus for measuring the state of an embedded microfiber would be similar in function to a metal detector used for finding buried objects. The metal detector uses three coils: one to generate the probing magnetic field that extends into the ground, a reference coil to cancel the probe field, and a measurement coil to sense small magnetic fields associated with eddy currents induced in any buried metallic object. Figure 23 shows a concept arrangement for a hand held device capable of measuring the response of an embedded microfiber sensor in a composite or fabric structure. The measuring system consists of a stack of three coils where the source coil is shown in red, the reference coil in green, and the measurement coil in blue. The source coil generates the input field that excites the microfiber while the measurement coil senses the microfiber response, and the reference coil cancels the source coil signal (see close-up

in figure 23). As in the earlier measurement apparatus, the reference coil and the measurement coil are identical but wired in opposition. The reference coil is located such that it measures the input signal but not the microfiber response signal, with the resultant measured output being: $H_m = H_{in} + (-H_{in}) + H_m$.

The device uses a universal joint that allows three-dimensional rotation of the coils. To be practical, the measuring device must be hand held and the approximate locations of the embedded microfibers be known to its user. The response range of a typical microfiber is short, so sensor locations must be spaced to prevent multiple microfibers from interfering with one another. The required minimum spacing between embedded microfibers has not been determined. A health status inspection would consist of bringing the hand-held device's crosshairs to the region where the microfiber was installed, choose the appropriate orientation (x, y or z) and measure the microfiber response. A return signal from the microfiber indicates that it is intact and the panel or structure has not undergone excessive loading. If no signal or a distorted signal appears, then the operator knows that the particular microfiber has undergone considerable stress and the region or panel associated with that microfiber is suspect and should be replaced or repaired. Figure 24 shows a NASA astronaut measuring the structural integrity of an airlock on a DSH due to an external impact; such measurements could also be made from the interior of the DSH. The orientation of the installed microfiber sensor (x, y, z) determines the orientation of the instrument head with the X orientation as illustrated in the figure.
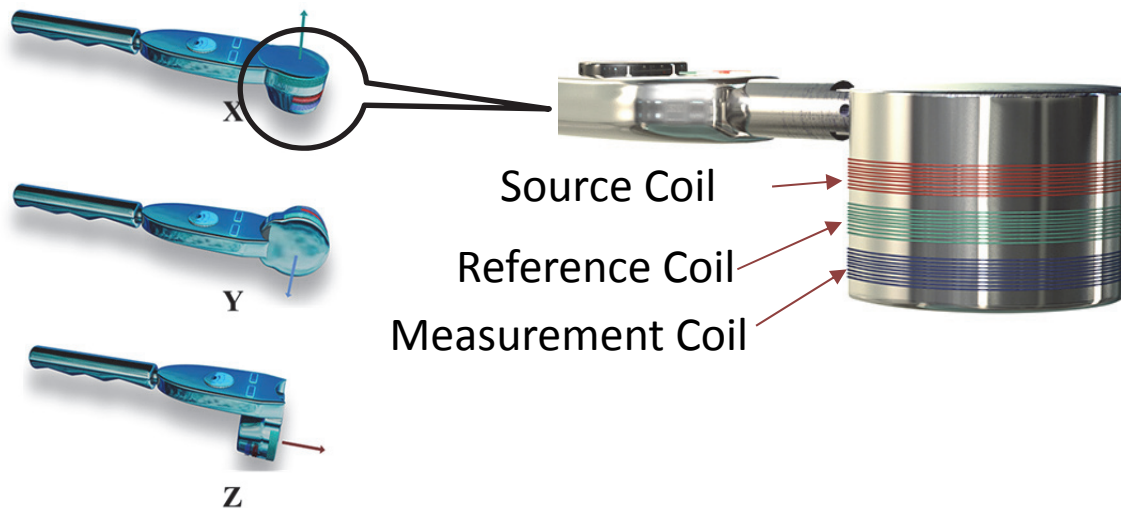
Figure 23. Proposed Hand-Held Apparatus for Monitoring Microfiber Health (with Three-Coil Arrangement Shown in the Closeup)
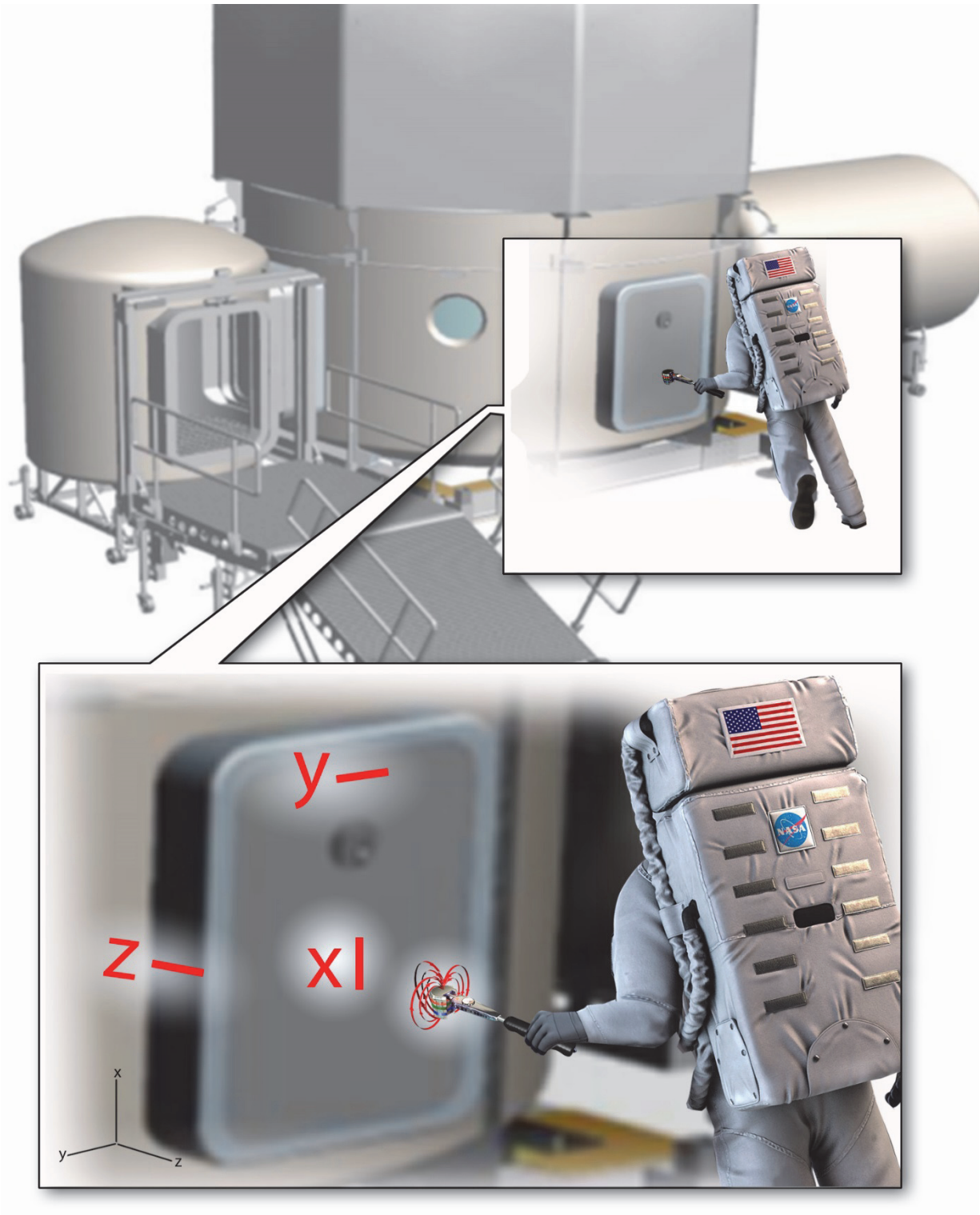
Figure 24.   NASA Astronaut Measuring the Integrity of a Habitat's Airlock

REFERENCES

1. K. Mohri, F.B. Humphrey, J. Yamasaki, and K. Okamura, "Jitter-Less Pulse Generator Elements Using Amorphous BisTable Wires," *IEEE Transactions on Magnetics*, vol. MAG-20, no. 5, September 1984, pp. 1409–1411.

2. K. Mohri, F.B. Humphrey, J. Yamasaki, and F. Kinoshita, "Large Barkhausen Effect and Matteucci Effect in Amorphous Magnetostrictive Wires for Pulse Generator Elements," *IEEE Transactions on Magnetics*, vol. MAG-21, no. 5, September 1985, pp. 2017–2019.

3. K. Mohri, F.B. Humphrey, K. Kawashima, K. Kimura, and M. Mizutani, "Large Barkhausen and Matteucci Effects in FeCoSiB, FeCrSiB, and FeNiSiB Amorphous Wires," *IEEE Transactions on Magnetics*, vol. 26, no. 5, pp. 1789–1791, September 1990.

4. L.V. Panina, M. Mizutani, K. Mohri, F.B. Humphrey and I. Ogasawara, "Dynamics and Relaxation of Large Barkhausen Discontinuity in Amorphous Wires," *IEEE Transactions on Magnetics*, vol. 27, no. 6, November 1991, pp. 5331–5333.

5. K. Mohri, "Review on Recent Advances in the Field of Amorphous-Metal Sensors and Transducers," *IEEE Transactions on Magnetics*, vol. 20, no. 5, September 1984, pp. 942–947.

6. D. Mee, L. R. Mooney; L. N. Howell, Jr., M. R. Ellis, E. B. Ripley, and E. Garlea, "Amorphous Wire Sensor Applications and Limitations for State-of-Health Monitoring FY12 Report for PD100108," Y12 National Security Complex, Oak Ridge, TN, 37831-8169, September 2012.

7. Smith, Langford, Hagen, Working, Cavallaro & Bruno, Gordon, "Overview of Evolved Secondary Structural Prototypes in Support of the Deep Space Habitat with Material and Sensor Strands Development," NASA Langley Report (in preparation).

8. P. Cavallaro, "Investigation of Conceptual Inflatable Fabric Structures for Use as Protective Crew Quarter Systems in Space Vehicles and Space Habitat Structures," NUWC-NPT Technical Report 12,179, Naval Undersea Warfare Center Division, Newport, RI, 30 June 2015.

9. P. Rudkowski, G. Rudkowska, and J.O. Strom-Olsen, "The Fabrication of Fine Metallic Fibers by Continuous Melt-Extraction and their Magnetic and Mechanical Properties," *Materials Science and Engineering*, no. A133, 1991, pp. 158–161.

10. J. Strom-Olsen, "Fine Fibers by Melt Extraction," *Materials Science and Engineering*, no. A178, 1994, pp. 239–243.

11. R. Becker and W. Döring, *Ferromagnetismus*, Springer, Berlin, Germany, 1939.

REFERENCES (Cont'd)

12. H. Hauser and P. Ripka, *Magnetic Sensors and Magnetometers*, Artech House, Norwood, MA, 2000, pp. 13.

13. K. Mohri, F.B. Humphrey, L.V. Panina, Y. Honkura, J. Yamasaki, T. Uchiyama, and M. Hirami, "Advances of Amorphous Wire Magnetics Over 27 Years," *Physica Status Solidi (A)*, Applications And Materials Science, vol. 206, No. 4, 2009, pp. 601–607.

14. P. Ciureanu, Unpublished Data from the Laboratory of Magnetism, Ecole Polytechnique, Montreal, Canada, July 2010.

15. Private Communication with D. Mee, Y12 National Security Complex, September 2013.

16. Private Communication with R. Smith, NASA Langley, November 2014.

17. R. Smith, Proposed Ni/Co Fiber Strand Test Matrix, NASA Langley, 8 July 2013.

18. Private Communication with R. Smith, NASA Langley, August 2015.

INITIAL DISTRIBUTION LIST

Addressee	No. of Copies
Center for Naval Analyses	1
Defence Science and Technology Group—Maritime Division (D. Liebing, M. Steed)	2
Defense Technical Information Center (DTIC)	1
NASA, Langley Research Center (R. Smith)	20
Office of Naval Intelligence (C. Boswell)	1
Office of Naval Research (S. Potashnik, M. Wardlaw)	2
Raytheon Company (P. Corriveau)	1
Y12 National Security Complex (W. Barrett, D. Mee)	2